Published in final edited form as:
ACS Chem Biol. 2011 November 18; 6(11): 1257–1264. doi:10.1021/cb2002544.

Bacterial self-resistance to the natural proteasome inhibitor salinosporamide A

Andrew J. Kale[1], **Ryan P. McGlinchey**[1], **Anna Lechner**[1], and **Bradley S. Moore**[1,2,*]

[1]Center for Marine Biotechnology and Biomedicine, Scripps Institution of Oceanography, University of California at San Diego, 9500 Gilman Drive, La Jolla, California 92093

[2]Skaggs School of Pharmacy and Pharmaceutical Sciences, University of California at San Diego, 9500 Gilman Drive, La Jolla, California 92093

Abstract

Proteasome inhibitors have recently emerged as a therapeutic strategy in cancer chemotherapy but susceptibility to drug resistance limits their efficacy. The marine actinobacterium *Salinispora tropica* produces salinosporamide A (NPI-0052, marizomib), a potent proteasome inhibitor and promising clinical agent in the treatment of multiple myeloma. Actinobacteria also possess 20S proteasome machinery, raising the question of self-resistance. We identified a redundant proteasome β-subunit, SalI, encoded within the salinosporamide biosynthetic gene cluster and biochemically characterized the SalI proteasome complex. The SalI β-subunit has an altered substrate specificity profile, 30-fold resistance to salinosporamide A, and cross-resistance to the FDA-approved proteasome inhibitor bortezomib. An A49V mutation in SalI correlates to clinical bortezomib resistance from a human proteasome β 5-subunit A49T mutation, suggesting that intrinsic resistance to natural proteasome inhibitors may predict clinical outcomes.

Keywords

actinomycete; bortezomib; 20S proteasome; salinosporamide; self-resistance

The 26S proteasome is a macromolecular enzymatic complex responsible for the regulated hydrolysis of cellular proteins that in turn mediates processes such as amino acid recycling, cell cycle control, cell differentiation, and apoptosis (1). Ubiquitinated proteins are targeted by the 19S regulatory cap and transferred into the interior of the cylindrical 20S proteasome core particle for degradation by catalytic β-subunits having nucleophilic *N*-terminal threonine residues (1). Eukaryotes harbor a two-fold symmetrical $\alpha_{(1–7)}\beta_{(1–7)}\beta_{(1–7)}\alpha_{(1–7)}$ barrel-shaped 20S structure with three active β-subunits (β 1, caspase-like (C-L); β 2, trypsin-like (T-L); and β 5, chymotrypsin-like (CT-L)) that display distinct proteolytic specificities (2). Their catalytic inhibition with mechanism-based small molecules has exposed the proteasome as an important therapeutic target in cancer and inflammation (3). Recently the dipeptide boronic acid bortezomib (**1**, Figure 1) was approved by the FDA for the treatment of relapsed multiple myeloma and mantle cell lymphoma as a first in class proteasome inhibitor (PI) that functions as a reversible inhibitor of the β 5-subunit (4,5). Acquired resistance to bortezomib, however, has already emerged and limits its pronounced clinical benefit that in part is due to point mutations in the proteasome β 5-subunit (6–9).

*Corresponding author: bsmoore@ucsd.edu.

ASSOCIATED CONTENT

Supporting Information Available: This material is available free of charge *via* the Internet at http://pubs.acs.org.

Salinosporamide A (**2**), a potent PI naturally synthesized by the marine bacterium *Salinispora tropica*, represents an alternative treatment option due to its distinct chemical structure and mechanism of action (10). Its biosynthesis in an actinobacterium, which is unique amongst bacterial divisions to maintain a 20S proteasome (1), with a simplified $\alpha_7\beta_7\beta_7\alpha_7$ structure, raises the question of the molecular basis behind natural proteasome resistance and whether this mechanism correlates to clinical drug resistance. Unlike the eukaryotic 26S proteasome which is essential for survival (11), the 20S proteasome has been inactivated in several actinobacteria without loss of viability (12,13). *Mycobacterium tuberculosis* is a notable exception that requires the proteasome for pathogenicity in response to host induced oxidative stress (14). The recent discovery of the prokaryotic ubiquitin-like protein (PUP) has established that the actinobacterial proteasome regulates the controlled destruction of targeted proteins (15– 18). Elucidating the specific proteins and pathways regulated by the 20S proteasome in actinobacteria remains an active area of investigation.

Salinosporamide A belongs to a growing family of potent natural PIs that also includes the actinomycete natural products lactacystin, cinnabaramide A, epoxomicin, and belactosine A (10,19). However, despite the many examples of natural product PIs being produced by microbes that must maintain their own functional proteasomes, the biochemical basis for natural resistance has not been defined. We describe here the identification and characterization of a 20S proteasome target modification resistance mechanism to salinosporamide A in the producing organism *S. tropica.*

RESULTS AND DISCUSSION

Identification of a transcriptionally active 20S proteasome β-subunit in the salinosporamide biosynthetic gene cluster

We recently sequenced the complete genome of *S. tropica* CNB-440 and functionally characterized the salinosporamide A gene locus (20,21). Curiously, towards one end of the 41-kb *sal* gene cluster resides the gene *salI* (Strop_1015) encoding a proteasome β-subunit. Its physical location in a biosynthetic operon associated with a PI strongly suggested its involvement in resistance through target modification, a strategy more commonly associated with antibiotic resistance (22). Further genomic analysis of *S. tropica* CNB-440 identified a typical actinobacterial 20S proteasome gene cluster (Strop_2241–2247) that includes adjacent genes encoding α and β proteasome subunits. We reasoned that the SalI β-subunit would additionally complex with the lone α-subunit during the biosynthesis of salinosporamide A to render a functional 20S proteasome with greater tolerance to the PI. To this end, we analyzed mRNA transcripts of *Strop_2245* (α-subunit), *Strop_2244* (β-subunit), *salI*, and the salinosporamide biosynthesis gene *salL* as a reference to correlate SalI to inhibitor production. We observed active transcription of *salI* in parallel to the proteasome α and β subunits and *salL* (Figure 2a), suggesting that SalI has the potential to form an active proteasome complex during salinosporamide A biosynthesis.

In vitro characterization of *S. tropica* proteasome complexes

To generate homogeneous proteasome complexes for *in vitro* analysis, we heterologously expressed proteasome subunits in *Escherichia coli*, which lacks an endogenous 20S proteasome. Individually expressed Strop_2244 β-subunit (referred to henceforth as β_1) and SalI remained insoluble until complexed with the α-subunit, suggesting a mutual dependence for correct folding. Coexpression of the readily soluble α-subunit as an *N*-terminal His_6-tagged protein (29.1 kDa) with untagged β_1 or SalI (23.4 and 24.6 kDa, respectively, after prosequence removal) and purification of the respective complexes by Ni^{2+} affinity chromatography and size-exclusion chromatography gave protein bands in

excess of 669 kDa (Figure 2b), which was consistent with fully assembled $\alpha_{7(}\beta_{1)7(}\beta_{1)7}\alpha_{7}$ (ca. 735 kDa) and α_7SalI$_7$SalI$_7\alpha_7$ (ca. 752 kDa) proteasome complexes. Proteolytic activity of these bands was verified by the application of a fluorogenic peptide-7-amino-4-methylcoumarin (amc) substrate directly to the gel (Figure 2c). We next explored the respective hydrolytic activities and substrate specificities of the purified proteasome complexes using an array of peptide-amc substrates (Table 1). The α/β_1 complex was most active against the T-L substrate Ac-RLR-amc with further activity against the CT-L substrate Suc-LLVY-amc and the general substrate Z-VKM-amc. For the α/SalI complex, T-L activity was abolished while that of CT-L was highly reduced. Instead, the α/SalI complex was 6-fold more active against Z-VKM-amc than with CT-L substrate Suc-LLVY-amc, which is often preferred by other actinobacterial proteasomes (23–26). We thus observed a markedly different substrate specificity between the two complexes in which the α/SalI complex was approximately 5-fold less active than the α/β_1 complex with the substrates evaluated.

We next interrogated the α/β_1 and α/SalI complexes against salinosporamide A inhibition to explore their relevant tolerance. As hypothesized, we observed a 16–30 fold increase in IC50 with the α/SalI complex in comparison to the α/β_1 complex (Table 2). Both proteasome complexes exhibited time-dependent inhibition by salinosporamide A (Supplementary Figure 1) and no recovery of proteolytic activity was observed after buffer exchange to remove salinosporamide A. The resistance of the α/SalI complex to inhibition was conserved with the reversibly-inhibiting descholoro analog salinosporamide B (**3**) (27) and the structurally distinct bortezomib, showing 7 and 13 fold increases in IC_{50} values, respectively (Table 3). The resistance to both salinosporamide A and bortezomib, combined with the marked shift in proteolytic specificities, indicated that β_1 and SalI have significant differences in substrate binding pocket dynamics.

Probing proteasome binding pocket residues with mutational analysis

To gain insight into the molecular basis governing SalI's PI resistance, we scrutinized its amino acid residues lining the conserved S1 and S2 pockets since the compact nature of salinosporamide restricts its proteasome binding interactions to these sites. Crystallographic analysis of salinosporamide A bound to the β 5-subunit of the *Saccharomyces cerevisiae* proteasome previously revealed beneficial hydrophobic interactions between its cyclohexenyl side chain and several residues of the S1 binding pocket, most notably Met45, yet minimal contact with the S2 pocket (27). Alignment of β_1, SalI, β 5 from *S. cerevisiae* and *Homo sapiens,* and previously characterized actinobacterial proteasome β-subunits revealed that SalI possesses unique Phe45 and Val49 residues, both located within the S1 binding pocket (Figure 3a). Position 45 forms the base of the S1 binding pocket and is known to confer CT-L, T-L, or C-L preference to the eukaryotic β-subunits, while position 49 resides at the entrance of the pocket (Figure 3b) (2). We thus targeted both positions by site-directed mutagenesis and generated mutants in which we exchanged their residues in order to investigate substrate specificity and salinosporamide resistance in both *S. tropica* β-subunits, β_1 and SalI.

Mutagenesis of the β_1 Met45 residue, which is conserved in the *S. cerevisiae* and human β 5-subunits where it contributes to their CT-L activities, to Phe as in SalI resulted in the α/β_1 M45F mutant that maintained its native proteolytic activity (Table 1) and sensitivity to salinosporamide A (Table 2). Conversely, the α/SalI F45M mutant had significantly greater hydrolytic activity for its substrates Suc-LLVY-amc and Z-VKM-amc at ~10 and 4 times, respectively, its native activity (Table 1). This mutant did not engender new activity against the five previously tested inactive substrates, revealing that substrate specificity was not altered as originally envisaged, just its catalytic efficiency. Further, α/SalI F45M was

slightly more resistant to salinosporamide A than the native α/SalI complex (Table 2), indicating that position 45 is not a major determinant in salinosporamide A resistance.

We rather hypothesized that position 49 contributes to salinosporamide resistance as the substitution of the larger Val residue in SalI for the conserved Ala residue that typifies β-subunits would constrict the S1 binding pocket and hinder inhibitor binding. Previously an A49V mutation was identified in the *S. cerevisiae* β 5-subunit that resulted in a shift of substrate specificity away from CT-L activity (28). Similar A49T acquired mutations in human monocytic/macrophage, multiple myeloma, and lymphoblastic Jurkat T cell lines were recently shown to confer resistance to bortezomib and cross-resistance to other peptide-based PIs (7–9). We thus first generated the α/β_1 A49V mutant. This mutant lost most of its hydrolytic activity while maintaining Z-VKM-amc activity, albeit at reduced levels (Table 1). When incubated with salinosporamide A, we observed greater than a ten-fold increase in its IC_{50} (Table 2). Unfortunately, our attempts to further correlate the role of Val49 in salinosporamide resistance with α/SalI V49A were unsuccessful since this mutant complex lost its hydrolytic activity. Denaturing PAGE revealed a 2–3 kDa increase in the SalI subunits containing the V49A mutation, indicating activity was lost due to improper prosequence cleavage (Figure 2d). The α/β_1 M45F/A49V and α/SalI F45M/V49A double mutants behaved similarly to the respective position 49 single mutants, indicating that this residue is significantly more influential to S1 binding pocket dynamics in both complexes.

The mechanism of self-resistance to endogenously produced salinosporamide A in *S. tropica* appears to have independently evolved in human cancer cell lines with prolonged exposure to the drug. Intriguingly, acquired human resistance to a natural anticancer agent that mirrors the evolved natural resistance strategy was also recently described for the topoisomerase I inhibitor camptothecin. In this case, the camptothecin-containing medicinal plant carries a point mutation in the encoding topoisomerase I gene that is identical to one found in resistant human cell lines (29). However, there is a subtle difference in the salinosporamide and camptothecin resistance examples since camptothecin is produced by an endophytic fungus associated with the plant (30), and thus genes for biosynthesis and resistance are rather decoupled between the producer and the resistant host.

Targeting SalI for inhibition with modified P1 residues

Mutational analysis revealed the SalI A49V mutation to be the primary driver of salinosporamide A resistance. The observed cross-resistance to bortezomib, bearing a P1 leucine residue, and decreased activity with the CT-L substrate suggested that Val49 diminishes the potent inhibition of salinosporamide A via S1 binding pocket constriction. To probe this premise, we further interrogated the *S. tropica* 20S proteasome complexes with salinosporamide derivatives bearing modified C-5 residues corresponding to the P1 site. We thus assayed four salinosporamide X derivatives previously generated by mutasynthesis (31) in which the cyclohexenyl ring of salinosporamide A was replaced with smaller (antiprotealide (**4**), salinosporamides X3 (**5**) and X7 (**6**)) or more flexible (salinosporamide X5 (**7**)) aliphatic P1 residues. In each case, we measured a loss in proteasome inhibition in relation to salinosporamide A (Table 3), suggesting a more complicated picture in inhibitor binding and S1 pocket dynamics.

Survey of secondary proteasomal β-subunits in Actinomycetes

Having validated the relationship between the endogenous *S. tropica* PI salinosporamide and the resistance proteasome β-subunit SalI, we next probed other actinobacterial genomes for similar associations in order to query whether this is a common phenomenon for PI biosynthesis. Since salinosporamide A is structurally related to the PIs salinosporamide K (**8**) from "*Salinispora pacifica*" strain CNT-133A (32) and the cinnabaramides (**9**) from

Streptomyces sp. JS360 (33), we first probed their biosynthetic loci. We cloned and partially sequenced the cinnabaramide biosynthetic gene cluster and identified an associated *salI* homolog (46% sequence identity) whose product has the resistance Phe45/Val49 sequence signature (Table 4). The complete cinnabaramide biosynthetic cluster, including this 20S proteasome β-subunit (CinJ), has been independently published (34). As in the case with *S. tropica*, *S.* sp. JS360 also harbors a primary 20S proteasome gene cluster that includes a β-subunit containing residues Ile45 and Ala49, which is consistent with previously characterized actinobacterial β-subunits (23–26). Sequence analysis of the recently sequenced "*S. pacifica*" salinosporamide K biosynthetic gene cluster, on the other hand, did not reveal an associated proteasome β-subunit, which may correlate with salinosporamide K's lower biosynthetic titer and diminished inhibitory activity (32).

BLAST analysis of the *S. tropica* β_1-subunit against all available actinobacterial genomes uncovered several organisms with dual proteasome β-subunits. Comparison of the primary and secondary proteasome β-subunits of *Streptomyces avermitilis* MA-4680, *Thermomonospora curvata* DSM 43183, and *Streptomyces bingchenggensis* BCW-1 showed that Ala49 is switched to either Val or Leu in one of the two subunits (Table 4). In two cases, Val49 occurs in the freestanding secondary β-subunit, as is the case with *S. tropica*, while the primary β-subunit of *S. bingchenggensis* contains Leu49. Further sequence analysis of the gene neighborhoods of the secondary proteasome β-subunits revealed in the case of *S. bingchenggensis* a hybrid nonribosomal peptide synthetase–polyketide synthase biosynthetic gene cluster (ADI05330/ADI05329) located immediately adjacent to its secondary β-subunit. This gene cluster is predicted to encode the biosynthesis of a tripeptide natural product with a modified *C*-terminal acetate extension. As many synthetic and natural PIs are short peptides with an electrophilic modification at the *C*-terminus (19), we anticipate that this cluster encodes an orphan PI with a novel peptidic structure. This clear association of a secondary proteasome β-subunit with a natural product biosynthetic gene cluster may signal a new experimental paradigm for the discovery of natural PIs.

CONCLUSIONS

The recruitment of a pathway specific proteasome β-subunit to assemble with the primary α-subunit to form a 20S proteasome complex (α/SalI) that is both hydrolytically active and relatively resistant to PIs is unprecedented and defines a new mechanism of natural product resistance. This evolved resistance mechanism in a PI-producing microbe is strikingly similar to the analogous target modification paradigm recently reported for bortezomib treatment in human cancer cell lines, thereby suggesting that natural PI chemotherapy, which includes salinosporamide A, may ultimately be similarly susceptible to acquired resistance by proteasome modification.

METHODS

Materials

Salinosporamides A and B were purified from cultures of *S. tropica* CNB-440 (35). Proteasome inhibitors of the salinosporamide X series were produced and purified from a genetically modified *S. tropica* strain as previously described (31,36). All chemicals purchased were of the highest quality. Proteasome inhibitor Velcade® (Bortezomib) was purchased from LC Laboratories and the seven 7-amino-4-methylcoumarin (amc) tagged peptide substrates were purchased as follows: substrates Z-Val-Lys-Met-amc, Z-Leu-Leu-Leu-amc, Suc-Leu-Leu-Val-Tyr-amc, MeOSuc-Ala-Ala-Pro-Val-amc, Ac-Arg-Leu-Arg-amc, and Z-Leu-Leu-Glu-amc from Enzo Life Sciences and substrate Suc-Ala-Pro-Ala-amc from Peptides International, Inc.

mRNA transcript analysis

Total RNA was extracted from *S. tropica* CNB-440 and converted to cDNA as reported previously (21). PCR was run for 25 cycles using Taq polymerase (New England Biolabs) and 500 ng of cDNA in 10 μL reactions. Primers used were: *salL*, forward 5′ TCGTGGACATAACCCATGAC 3′ and reverse 5′ AGGACCTCGTGACACTCGAC 3′; *salI*, forward 5′ TAGTCGTCCGTGATCGTGAG 3′ and reverse 5′ GCCGTCCACGTTCTTAACAT 3′; Strop_2244, forward 5′ CTGGAGCACTACGAGAAGAC 3′ and reverse 5′ GTCACGTCGAAGCTGAAG 3′; and Strop_2245, forward 5′ CCTGAACGGTCTGAGCTAC 3′ and reverse 5′ GGTACAGTTCGTCGTCCTC 3′. PCR products were approximately 250 bp in size.

Plasmid construction

Proteasome α (Strop_2245, accession: YP_001159073) and β_1 (Strop_2244, accession: YP_001159072) or SalI (Strop_1015, accession: YP_001157868) subunits were sequentially cloned from genomic DNA of *S. tropica* CNB-440 into the ampicillin resistant pETDuet-1 coexpression vector (EMD Chemicals) to generate α/β_1 pETDuet and α/SalI pETDuet. The α-subunit contained an N-terminal His_6 tag while the β_1 and SalI subunits were untagged. An additional β_1-subunit was cloned into the kanamycin resistant pHIS8 expression vector (37). PCR reactions used *Pfu* Turbo DNA polymerase and were sequenced by Seqxcel, Inc.

The β_1-subunit was amplified for the pHIS8 vector with the primers: forward 5’ CCCATGGCGGATCC**GTG**GCAGCGGCTTTCGACC 3’ and reverse 5’ CCCATGGCGAATTC**TCA**GCCGCCCGGATTCTCC 3’. The α-subunit was amplified for MCS1 of pETDuet-1 with the primers: forward 5’ CACAGCCAGGATCCG**GTG**GCCATGCAGTTCTACGCC 3’ and reverse 5’ CCCATGGCGAATTC**CTA**GGGGGCCTCGGAATCGG 3’. β_1 was amplified for MCS2 of pETDuet-1 with the primers: forward 5’ GAGATATACAT**ATG**GCAGCGGCTTTCGACCCATC 3’ and reverse 5’ CCCATGGCGATATC**TCA**GCCGCCCGGATTCTCC 3’. SalI was amplified for MCS2 of pETDuet-1 with the primers: forward 5’ GAGATATACAT**ATG**AATCGGGGTCTGCCGTCCAC 3’ and reverse 5’ CCCATGGCGATATC**TCA**GGACGCGGTAAAGCTTCG 3’. The introduced BamHI, EcoRI, NdeI and EcoRV sites are underlined. The start and stop codons are shown in bold.

Site-directed mutagenesis

Site-directed mutagenesis was performed using the Stratagene Quikchange kit (Agilent Technologies). Single point mutations were performed using the α/β_1 pETDuet and α/SalI pETDuet constructs as templates to generate α/β_1 M45F pETDuet, α/β_1 A49V pETDuet, α/SalI F45M pETDuet, and α/SalI V49A pETDuet. Positions 45 and 49 refer to the amino acid position of the β_1 or SalI subunit from Thr1 after prosequence cleavage. Double mutations were performed sequentially. The α/β_1 M45F pETDuet plasmid was used as a template to generate the α/β_1 M45F/A49V double mutant while the α/SalI F45M pETDuet plasmid was similarly used to generate the α/SalI F45M/V49A double mutant. Both subunits of the mutant vectors were resequenced for verification following mutagenesis.

Primers sequences used were as follows with mutation sites underlined: α/β_1 M45F forward 5' CTCCCTGGTGGGCTTCGCGGGTGCCGCC 3' and reverse 5' GGCGGCACCCGCGAAGCCCACCAGGGAG 3'; α/β_1 A49V forward 5' CATGGCGGGTGCCGTCGGAATCGGGATC 3' and reverse 5' GATCCCGATTCCGACGGCACCCGCCATG 3'; α/β_1 M45F/V49A (from α/β_1 M45F) forward 5' CTTCGCGGGTGCCGTCGGAATCGGGATC 3' reverse 5' GATCCCGATTCCGACGGCACCCGCGAAG 3'; α/SalI F45M forward 5'

CTATTCGGCGGTCGGTATGGCCGGCACGGTGGGC 3' and reverse 5' GCCCACCGTGCCGGCCATACCGACCGCCGAATAG 3'; α/SalI V49A forward 5' GTTTCGCCGGCACGGCAGGCATCTCCATTGAC 3' and reverse 5' GTCAATGGAGATGCCTGCCGTGCCGGCGAAAC 3'; α/SalI F45M/V49A (from α/SalI F45M) forward 5' GTATGGCCGGCACGGCAGGCATCTCCATTGAC 3' and reverse 5' GTCAATGGAGATGCCTGCCGTGCCGGCCATAC 3'.

Protein expression

All expression vectors were transformed into *Escherichia coli* BL21 (DE3). To increase titers of the α/β_1 wild-type complex, a second β_1 expression plasmid, β_1 pHIS8, was transformed concurrently with α/β_1 pETDuet. A 10 ml culture in LB broth containing 100 μg ml^{-1} ampicillin was grown overnight at 37 °C. This was used to inoculate a 1 L culture of ZY media with autoinduction containing 100 μg ml^{-1} ampicillin (38). In the case of the wild-type α/β_1 proteasome expression, 50 μg ml^{-1} kanamycin was also added to starter and expression cultures. Expression cultures were grown on an orbital shaker for 20 h at 28 °C.

Protein purification

All protein purification steps took place at 4 °C. Protein purification buffers contained 300 mM NaCl, 50 mM sodium phosphate adjusted to pH 8.0, and increasing concentrations of imidazole. Buffers A (lysis), B (wash), and C (elution) contained 10, 20, and 250 mM imidazole, respectively. Cells were pelleted at 6,300 g for 15 min, resuspended in buffer A and lysed with six 30 sec bursts of probe sonication with resting periods of 30 sec. The lysate was centrifuged for 45 min at 20,000 g. Soluble protein was collected and equilibrated with Ni-NTA resin for 1 h before it was purified by Ni-NTA affinity chromatography, washed with several volumes of buffer B and eluting with 10 ml of buffer C. Washed and eluted protein was concentrated with a Vivaspin 100 kDa cut-off spin concentrator (GE biosciences) and resuspended in 100 mM Tris-HCl at pH 8.0. Concentrated protein was further purified by size exclusion chromatography on a HiLoad 16/60 Superdex 200 column (GE biosciences) with a 100 mM Tris-HCl pH 8.0 mobile phase and reconcentrated with a vivaspin 100 kDa cutoff protein concentrator.

Native gel analysis and fluorescent overlay assay

10 μg α/β_1 or 10 μg α/SalI were loaded onto an Invitrogen (4–16%) NativePAGE gel (Life Technologies). The gel was run at 150 V at 4 °C. For direct band visualization, the gels were washed and stained with Coomassie Brilliant Blue. For fluorescent visualization assays, the unstained native gel was briefly washed with H_2O then submerged in 25 μM Suc-LLVY-amc containing 50 mM Tris-HCl pH 8.0 buffer solution and shaken at room temperature for 60 minutes in darkness. The gel was transilluminated at 360 nm using a Gel Logic 2200 gel imager (Carestream). For salinosporamide inhibition, proteasome was incubated with 75 μM salinosporamide A for 20 min prior to loading of the gel.

Denaturing gel analysis

Protein samples were prepared for denaturing PAGE by boiling for 5 min prior to loading 5–15 μg proteasome onto the gel. Samples were loaded onto an Invitrogen NuPAGE 16% Tris-glycine SDS gel and run at 125 V for 3 h. Gels were washed and stained with Coomassie brilliant blue.

Proteasome assays

All proteasome assays were performed at a final volume of 50 μL in Greiner half-well microplates at 30 °C in 50 mM Tris-HCl pH 8.0, unless otherwise specified. Fluorescence

was measured on a Spectramax M2 plate reader (Molecular Devices) with an excitation wavelength of 355 nm and an emission wavelength of 460 nm.

Rates of hydrolysis

Purified proteasome complexes were assayed at three concentrations, each in triplicate. Enzyme concentrations assayed varied by proteasome complex from 5–60 μg ml^{-1} depending on activity. Substrate was added to 40 μM. Change in fluorescence was monitored continuously and the slope of the steady state portion of the curve was used to calculate the hydrolysis rate at that enzyme concentration. The average hydrolysis rate at each enzyme concentration was then plotted and a line was fit to obtain the hydrolysis rate per enzyme concentration (39). Relative fluorescence units were converted to μM by comparison to a standard curve of 7-amino-4-methylcoumarin in 50 mM Tris-HCl pH 8.0.

Proteasome inhibition

Proteasome complexes were incubated in serial dilutions of the proteasome inhibitors for 15 min at 30 °C. Enzyme concentration was adjusted between 1–3 μg per reaction (20–60 μg ml^{-1}) to ensure adequate activity for measurement of inhibition. Amounts of proteasome added per reaction were: 1.2 μg α/β_1, 1.3 μg α/β_1 F45M, 1.0 μg α/β_1 A49V, 3.0 μg α/β_1 M45F/V49A, 1.7 μg α/SalI, and 2.9 μg α/SalI F45M. The α/SalI V49A and α/SalI F45M/V49A mutants were not tested due to lack of hydrolytic activity. Fluorogenic substrate was then added to 40 μM and the reaction allowed to proceed for 30 min in darkness before fluorescence was measured. Maximum activity was set as proteasome in the absence of inhibitor and minimum activity was set as fluorogenic substrate in the absence of proteasome. Measurements were performed in triplicate and averaged. IC_{50} values were calculated from 4-parameter logistic curve fittings (39).

Time-dependence of inhibition

Dilutions of salinosporamide A or B ranging from 0.5–100 μM and 40 μM Z-VKM-amc substrate (final concentrations) were warmed to 30 ºC in a 96-well plate. Pre-warmed α/β_1 or α/SalI was then added at 20 μg ml^{-1} (27 nM, 14 active sites) final concentration and fluorescence was measured every minute for 3.5 h at a constant temperature of 30 ºC.

Irreversibility of inhibition

To assess the reversibility of salinosporamide A inhibition on the α/β_1 and α/SalI complexes, 300 μl of 20 μg ml^{-1} enzyme in 50 mM Tris-HCl pH 8.0 buffer was incubated with 250 μM salinosporamide A or an equivalent amount of DMSO for 1.5 h at 30 ºC. Samples were buffer exchanged three times on Amicon Ultra 0.5ml 30 kDa cutoff centrifugal filters (Millipore) to remove inhibitor and added to a microplate containing 40 μM Z-VKM-amc substrate. Fluorescence was monitored at 30 ºC every minute for 3 h.

Cinnabaramide biosynthetic gene cluster cloning

DNA isolation and manipulations in *E. coli* and *Streptomyces* sp. JS360 were carried out according to standard methods (40,41). PCR amplifications were carried out using Taq DNA polymerase (Fermentas). Fosmid sequencing was conducted by GenoTech Corp. A genomic fosmid library of *S.* sp. JS360 was constructed in pCC2 (Epicentre) according to manufacturer's protocol. This library was screened by colony PCR with degenerate ketosynthase primers based on five ketosynthase sequences: the tetronomycin synthase TetA from *Streptomyces* sp. NRRL 11266 (BAE93722), the tylactone synthase TylG from *Streptomyces fradiae* (O33954), the jamaicamide synthase JamE from *Lyngbya majuscula* (AAS98777), and the salinosporamide A and K synthase SalA and Sp_SalA from *Salinospora tropica* (ABP73645) and *Salinospora pacifica* (ADZ28493), respectively. The

primers were FP_KSdeg 5′ TGGGARGCDCTGGARGABGCBGGC 3′, with a degeneracy of 108, and RP_ KSdeg 5′ GCCGTYGGCDCGGGCGTCGAAGG 3′, with a degeneracy of 6. The *cinJ* gene sequence was obtained through gene walking from the 5'end of the *cinA* polyketide synthase.

Streptomyces sp. JS360 proteasome gene cloning

The α-subunit was cloned from *S.* sp JS360 genomic DNA using the forward 5′GTGTCGACGCCGTTCTATG 3' and reverse 5' GCTTGAACTTGCGCTGCTG 3' primers. Oligonucleotides were designed based on an alignment of α-subunit genes from *Streptomyces scabiei* 87.22, *Streptomyces avermitilis* MA-4680, *Streptomyces coelicolor* A3(2), *Streptomyces lividans* TK24, *Streptomyces griseus* NBRC 13350, and *Streptomyces ghanaensis* ATCC 14672. Specific primers were used subsequently to identify an appropriate fosmid, which was further used as template to obtain the primary proteasome β-subunit sequence through gene walking from the 5' end of the α-subunit.

Accession codes

The primary 20S proteasome α and β subunit of *S.* sp. JS360 were deposited in GenBank with the accession number JF970179. The cinnabaramide associated 20S proteasome β-subunit was deposited in GenBank with the accession number JF970180.

Supplementary Material

Refer to Web version on PubMed Central for supplementary material.

Acknowledgments

This work was supported by a grant from the NIH (CA127622) to B. S. M. and the Albert and Anneliese Konanz Foundation, Mannheim, a graduate fellowship to A. L.

References

1. Murata S, Yashiroda H, Tanaka K. Molecular mechanisms of proteasome assembly. Nat Rev Mol Cell Biol. 2009; 10:104–115. [PubMed: 19165213]
2. Groll M, Ditzel L, Lowe J, Stock D, Bochtler M, Bartunik HD, Huber R. Structure of 20S proteasome from yeast at 2.4 angstrom resolution. Nature. 1997; 386:463–471. [PubMed: 9087403]
3. Borissenko L, Groll M. 20S proteasome and its inhibitors: crystallographic knowledge for drug development. Chem Rev. 2007; 107:687–717. [PubMed: 17316053]
4. Bross PF, Kane R, Farrell AT, Abraham S, Benson K, Brower ME, Bradley S, Gobburu JV, Goheer A, Lee SL, Leighton J, Liang CY, Lostritto RT, McGuinn WD, Morse DE, Rahman A, Rosario LA, Verbois SL, Williams G, Wang YC, Pazdur R. Approval summary for bortezomib for injection in the treatment of multiple myeloma. Clin Cancer Res. 2004; 10:3954–3964. [PubMed: 15217925]
5. Groll M, Berkers CR, Ploegh HL, Ovaa H. Crystal structure of the boronic acid-based proteasome inhibitor bortezomib in complex with the yeast 20S proteasome. Structure. 2006; 14:451–456. [PubMed: 16531229]
6. Chauhan D, Li GL, Shringarpure R, Podar K, Ohtake Y, Hideshima T, Anderson KC. Blockade of Hsp27 overcomes bortezomib/proteasome inhibitor PS-341 resistance in lymphoma cells. Cancer Res. 2003; 63:6174–6177. [PubMed: 14559800]
7. Oerlemans R, Franke NE, Assaraf YG, Cloos J, van Zantwijk I, Berkers CR, Scheffer GL, Debipersad K, Vojtekova K, Lemos C, van der Heijden JW, Ylstra B, Peters GJ, Kaspers GL, Dijkmans BAC, Scheper RJ, Jansen G. Molecular basis of bortezomib resistance: proteasome subunit β 5 (*PSMB5*) gene mutation and overexpression of PSMB5 protein. Blood. 2008; 112:2489–2499. [PubMed: 18565852]

8. Lu SQ, Yang JM, Song XM, Gong SL, Zhou H, Guo LP, Song NX, Bao XC, Chen PP, Wang JM. Point mutation of the proteasome β 5 subunit gene is an important mechanism of bortezomib resistance in bortezomib-selected variants of Jurkat T cell lymphoblastic lymphoma/leukemia line. J Pharmacol Exp Ther. 2008; 326:423–431. [PubMed: 18502982]
9. Ri M, Iida S, Nakashima T, Miyazaki H, Mori F, Ito A, Inagaki A, Kusumoto S, Ishida T, Komatsu H, Shiotsu Y, Ueda R. Bortezomib-resistant myeloma cell lines: a role for mutated *PSMB5* in preventing the accumulation of unfolded proteins and fatal ER stress. Leukemia. 2010; 24:1506–1512. [PubMed: 20555361]
10. Gulder TAM, Moore BS. Salinosporamide natural products: potent 20S proteasome inhibitors as promising cancer chemotherapeutics. Angew Chem Int Ed. 2010; 49:9346–9367.
11. Hochstrasser M. Ubiquitin, proteasomes, and the regulation of intracellular protein degradation. Curr Opin Cell Biol. 1995; 7:215–223. [PubMed: 7612274]
12. Knipfer N, Shrader TE. Inactivation of the 20S proteasome in *Mycobacterium smegmatis*. Mol Microbiol. 1997; 25:375–383. [PubMed: 9282749]
13. Hong B, Wang LF, Lammertyn E, Geukens N, Van Mellaert L, Li Y, Anne J. Inactivation of the 20S proteasome in *Streptomyces lividans* and its influence on the production of heterologous proteins. Microbiology-Sgm. 2005; 151:3137–3145.
14. Darwin KH, Ehrt S, Gutierrez-Ramos JC, Weich N, Nathan CF. The proteasome of *Mycobacterium tuberculosis* is required for resistance to nitric oxide. Science. 2003; 302:1963–1966. [PubMed: 14671303]
15. Pearce MJ, Mintseris J, Ferreyra J, Gygi SP, Darwin KH. Ubiquitin-like protein involved in the proteasome pathway of *Mycobacterium tuberculosis*. Science. 2008; 322:1104–1107. [PubMed: 18832610]
16. Festa RA, McAllister F, Pearce MJ, Mintseris J, Burns KE, Gygi SP, Darwin KH. Prokayrotic ubiquitin-like protein (Pup) proteome of *Mycobacterium tuberculosis*. Plos One. 2010; 5:e8589. [PubMed: 20066036]
17. Watrous J, Burns K, Liu WT, Patel A, Hook V, Bafna V, Barry CE, Bark S, Dorrestein PC. Expansion of the mycobacterial "PUPylome". Mol Biosyst. 2010; 6:376–385. [PubMed: 20094657]
18. Poulsen C, Akhter Y, Jeon AH-W, Schmitt-Ulms G, Meyer HE, Stefanski A, Stuhler K, Wilmanns M, Song Y-H. Proteome-wide identification of mycobacterial pupylation targets. Mol Syst Biol. 2010; 6:article number 386.
19. Moore BS, Eustáquio AS, McGlinchey RP. Advances in and applications of proteasome inhibitors. Curr Opin Chem Biol. 2008; 12:434–440. [PubMed: 18656549]
20. Udwary DW, Zeigler L, Asolkar RN, Singan V, Lapidus A, Fenical W, Jensen PR, Moore BS. Genome sequencing reveals complex secondary metabolome in the marine actinomycete *Salinispora tropica*. Proc Natl Acad Sci U S A. 2007; 104:10376–10381. [PubMed: 17563368]
21. Eustáquio AS, McGlinchey RP, Liu Y, Hazzard C, Beer LL, Florova G, Alhamadsheh MM, Lechner A, Kale AJ, Kobayashi Y, Reynolds KA, Moore BS. Biosynthesis of the salinosporamide A polyketide synthase substrate chloroethylmalonyl-coenzyme A from S-adenosyl-L-methionine. Proc Natl Acad Sci U S A. 2009; 106:12295–12300. [PubMed: 19590008]
22. Hopwood DA. How do antibiotic-producing bacteria ensure their self-resistance before antibiotic biosynthesis incapacitates them? Mol Microbiol. 2007; 63:937–940. [PubMed: 17238916]
23. Pouch MN, Cournoyer B, Baumeister W. Characterization of the 20S proteasome from the actinomycete *Frankia*. Mol Microbiol. 2000; 35:368–377. [PubMed: 10652097]
24. Nagy I, Tamura T, Vanderleyden J, Baumeister W, De Mot R. The 20S proteasome of *Streptomyces coelicolor*. J Bacteriol. 1998; 180:5448–5453. [PubMed: 9765579]
25. Tamura T, Nagy I, Lupas A, Lottspeich F, Cejka Z, Schoofs G, Tanaka K, Demot R, Baumeister W. The characterization of a eubacterial proteasome: the 20S complex of *Rhodococcus*. Curr Biol. 1995; 5:766–774. [PubMed: 7583123]
26. Zuhl F, Tamura T, Dolenc I, Cejka Z, Nagy I, DeMot R, Baumeister W. Subunit topology of the *Rhodococcus* proteasome. FEBS Lett. 1997; 400:83–90. [PubMed: 9000518]
27. Groll M, Huber R, Potts BCM. Crystal structures of salinosporamide A (NPI-0052) and B (NPI-0047) in complex with the 20S proteasome reveal important consequences of β-lactone ring

opening and a mechanism for irreversible binding. J Am Chem Soc. 2006; 128:5136–5141. [PubMed: 16608349]

28. Richter-Ruoff B, Heinemeyer W, Wolf DH. The proteasome/multicatalytic-multifunctional proteinase. *In vivo* function in the ubiquitin-dependent *N*-end rule pathway of protein degradation in eukaryotes. FEBS Lett. 1992; 302:192–196. [PubMed: 1321727]
29. Sirikantaramas S, Yamazaki M, Saito K. Mutations in topoisomerase I as a self-resistance mechanism coevolved with the production of the anticancer alkaloid camptothecin in plants. Proc Natl Acad Sci U S A. 2008; 105:6782–6786. [PubMed: 18443285]
30. Puri SC, Verma V, Amna T, Qazi GN, Spiteller M. An endophytic fungus from *Nothapodytes foetida* that produces camptothecin. J Nat Prod. 2005; 68:1717–1719. [PubMed: 16378360]
31. Nett M, Guider TAM, Kale AJ, Hughes CC, Moore BS. Function-oriented biosynthesis of β-lactone proteasome inhibitors in *Salinispora tropica*. J Med Chem. 2009; 52:6163–6167. [PubMed: 19746976]
32. Eustáquio AS, Nam SJ, Penn K, Lechner A, Wilson MC, Fenical W, Jensen PR, Moore BS. The discovery of salinosporamide K from the marine bacterium "*Salinispora pacifica*" by genome mining gives insight into pathway evolution. ChemBioChem. 2011; 12:61–64. [PubMed: 21154492]
33. Stadler M, Bitzer J, Mayer-Bartschmid A, Muller H, Benet-Buchholz J, Gantner F, Tichy HV, Reinemer P, Bacon KB. Cinnabaramides A-G: analogues of lactacystin and salinosporamide from a terrestrial streptomycete. J Nat Prod. 2007; 70:246–252. [PubMed: 17249727]
34. Rachid S, Huo LJ, Herrmann J, Stadler M, Kopcke B, Bitzer J, Muller R. Mining the cinnabaramide biosynthetic pathway to generate novel proteasome inhibitors. ChemBioChem. 2011; 12:922–931. [PubMed: 21387511]
35. Feling RH, Buchanan GO, Mincer TJ, Kauffman CA, Jensen PR, Fenical W. Salinosporamide A: a highly cytotoxic proteasome inhibitor from a novel microbial source, a marine bacterium of the new genus *Salinospora*. Angew Chem Int Ed. 2003; 42:355–358.
36. McGlinchey RP, Nett M, Eustáquio AS, Asolkar RN, Fenical W, Moore BS. Engineered biosynthesis of antiprotealide and other unnatural salinosporamide proteasome inhibitors. J Am Chem Soc. 2008; 130:7822–7823. [PubMed: 18512922]
37. Jez JM, Ferrer JL, Bowman ME, Dixon RA, Noel JP. Dissection of malonyl-coenzyme A decarboxylation from polyketide formation in the reaction mechanism of a plant polyketide synthase. Biochemistry. 2000; 39:890–902. [PubMed: 10653632]
38. Studier FW. Protein production by auto-induction in high-density shaking cultures. Protein Expr Purif. 2005; 41:207–234. [PubMed: 15915565]
39. SigmaPlot. Vol. 11.0. Systat Software, Inc; San Jose, CA:
40. Sambrook, J.; Russell, D. Molecular Cloning: A Laboratory Manual. 3. Cold Spring Harbor Laboratory Press; Cold Spring Harbor, NY: 2001.
41. Kieser, T.; Bibb, MJ.; Buttner, MJ.; Chater, KF.; Hopwood, DA. Practical Streptomyces Genetics. John Innes Centre, Norwich; United Kingdom: 2000.

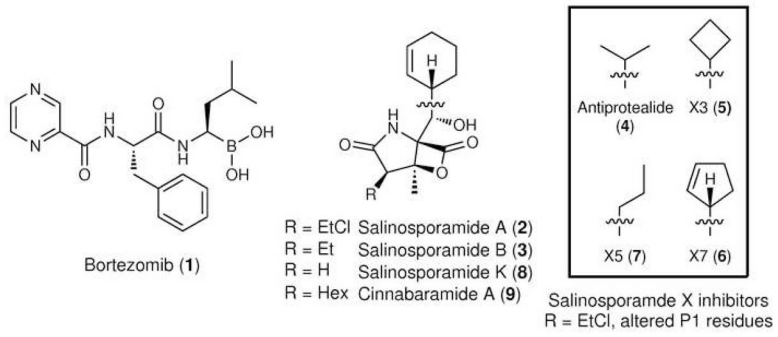

Figure 1.

Chemical structures of small molecule 20S PIs tested in this study. The respective P1 residues (Leu in bortezomib; cyclohexenyl in salinosporamides A, B, K, and cinnabaramide A; and the boxed residues in the salinosporamide X series) interact with the S1 specificity pocket of the proteasome β-subunit upon binding. The displaceable chloride of salinosporamide A confers irreversible inhibition.

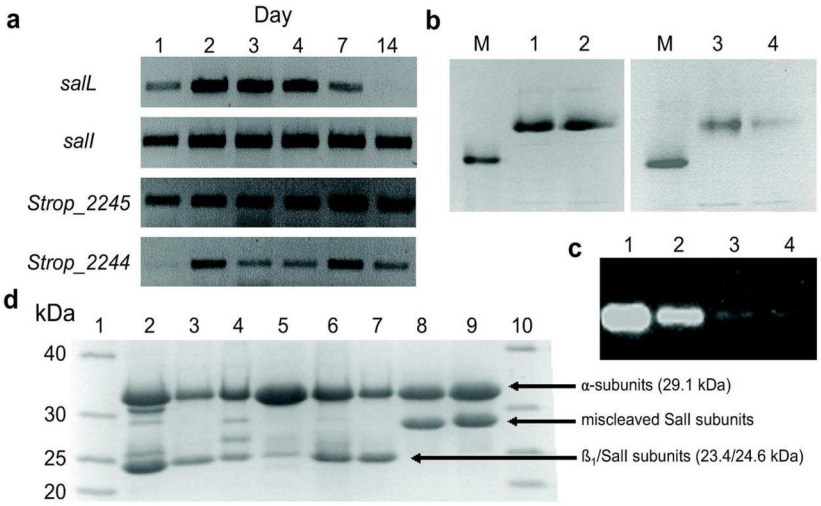

Figure 2.

Gel-based analysis of proteasomal transcription, heterologous expression, and subunit assembly. a) Proteasome transcriptional analysis in *S. tropica*. mRNA was isolated at multiple time points and transcripts of *salI*, *Strop_2245* (α-subunit), *Strop_2244* (β_1-subunit), and the salinosporamide chlorinase *salL* are shown. The *salI* gene is actively transcribed at all time points that salinosporamide A is being produced, as indicated by transcription of *salL*. Concurrent transcription of the α-subunit indicates that the α/SalI complex may form *in vivo* with salinosporamide production. b) Native PAGE analysis of the assembled proteasome complexes. Lanes: M, Thyroglobulin (669 kDa); 1, α/β_1; 2, α/β_1 pre-incubated with 75 μM salinosporamide A; 3, α/SalI; and 4, α/SalI pre-incubated with 75 μM salinosporamide A. Major bands above the 669 kDa marker correspond to fully assembled proteasome. c) Fully assembled proteasome bands, based on migration of and with the same lane assingments as (b), were visualized in overlay assays using the fluorogenic substrate Suc-LLVY-amc. d) Denaturing 16% SDS PAGE analysis of the proteasome complexes. Lanes: 1,10, NativeMark™ ladder; 2, α/β_1; 3, α/β_1 M45F; 4, α/β_1 A49V; 5, α/β_1 M45F/A49V; 6, α/SalI; 7, α/SalI F45M; 8, α/SalI V49A; and 9, α/SalI F45M/V49A. The increased size of SalI in lanes 8 and 9 indicate improper prosequence cleavage due to the V49A mutation.

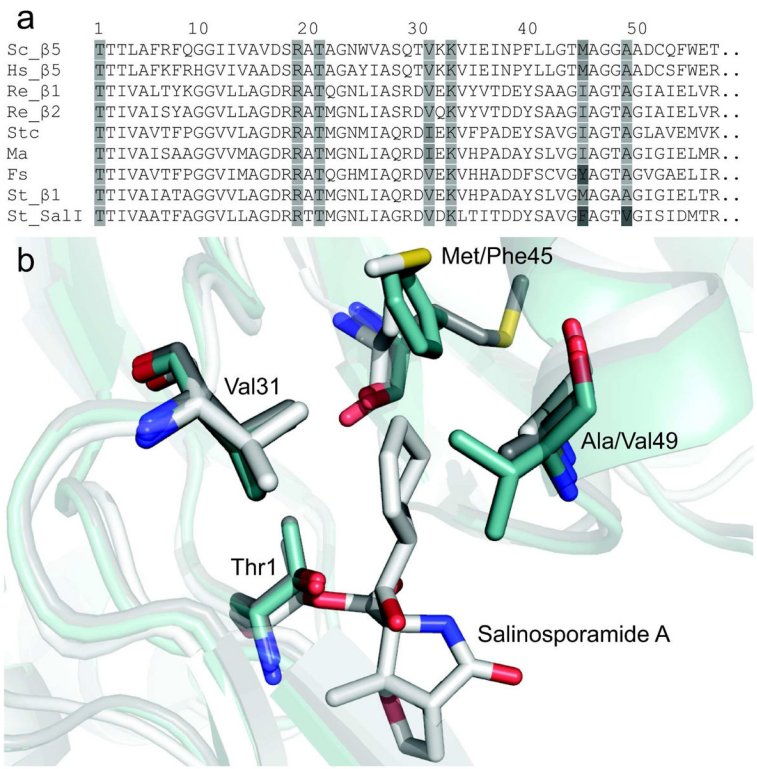

Figure 3.

Comparison of actinobacterial and eukaryotic β-subunit S1 binding pocket residues. a) A partial sequence alignment of characterized actinomycete β-subunits and the CT-L β5-subunits of *Saccharomyces cerevisiae* (Sc) and *Homo sapiens* (Hs) is shown from Thr1 to position 57. The actinobacterial β-subunits of *Rhodococcus erythropolis* PR4 (Re), *Streptomyces coelicolor* A3(2) (Stc), *Micromonospora aurantiaca* ATCC 27029 (Ma), *Frankia* sp. ACN14a (Fs), and *Salinispora tropica* CNB-440 (St) are displayed. Residues previously shown to interact with salinosporamide A during binding to the β5-subunit of *S. cerevisiae* are highlighted. Darker shades of gray indicate deviation from the consensus sequence. A full alignment is shown in the SI (Supplementary Figure 2). b) A structural depiction of salinosporamide A bound to the 20S proteasome. Residues forming the S1 binding pocket are shown. The Sc β5-subunit with salinosporamide A bound (white, PDB 2FAK chain K) is overlayed with β_1 (gray) and SalI (blue) of St, both homology modeled against the prokaryotic proteasome β-subunit of Re (PDB 1Q5Q chain H). The substitution of Phe45 and Val49 in SalI were predicted to alter substrate and inhibitor binding and therefore targeted for mutagenesis.

Table 1

Hydrolysis rates of *S. tropica* proteasome complexes for all active substrates[a]

	Hydrolysis rate (nmol hr^{-1} mg^{-1})		
Proteasome complex	**Suc-LLVY-amc**	**Ac-RLR-amc**	**Z-VKM-amc**
α/β_1	56.0 ± 1.3	93.8 ± 5.0	51.6 ± 2.7
α/β_1 M45F	46.9 ± 10.7	89.4 ± 6.6	53.8 ± 1.9
α/β_1 A49V	Inactive	Inactive	ND[b]
α/β_1 M45F/A49V	Inactive	Inactive	ND[b]
α/SalI	3.4 ± 0.2	Inactive	19.4 ± 0.6
α/SalI F45M	33.1 ± 2.5	Inactive	78.4 ± 0.3
α/SalI V49A	Inactive	Inactive	Inactive
α/SalI F45M/V49A	Inactive	Inactive	Inactive

[a] No activity was observed with substrates Z-LLL-amc, MeOSuc-AAPV-amc, Z-LLE-amc, and Suc-APA-amc. Data shown is the mean ± standard deviation, N = 3.

[b] Both α/β_1 A49V and α/β_1 M45F/A49V displayed detectable activity toward substrate Z-VKM-amc. However, these complexes were recovered in low yield and were prone to aggregation upon purification, therefore hydrolytic rates were not determined (ND).

Table 2

Salinosporamide A inhibition (IC_{50}) values for all wild-type and mutant complexes

Proteasome complex	Substrate[a]	IC_{50} (μM) salinosporamide A
α/$β_1$	LLVY	3.1 ± 0.2
	RLR	1.7 ± 0.8
	VKM	1.2 ± 0.1
α/$β_1$M45F	VKM	1.2 ± 0.1
α/$β_1$A49V	VKM	13.6 ± 2.2
α/$β_1$M45F/A49V	VKM	15.3 ± 2.2
α/SalI	LLVY	52.0 ± 3.5
	RLR	Inactive
	VKM	36.8 ± 2.4
α/SalI F45M	VKM	45.5 ± 2.3
α/SalI V49A	VKM	Inactive
α/SalI F45M/V49A	VKM	Inactive

[a] Substrate represents amino acid residues preceding fluorescent amc tag (ex. LLVY = Suc-LLVY-amc). Data shown is the mean ± standard deviation, N = 3.

Table 3

Inhibition (IC_{50}) values of wild-type α/β_1 and α/SalI proteasome complexes with various peptide-based inhibitors[a]

Inhibitor	α/β_1 IC_{50} (μM)	α/SalI IC_{50} (μM)
Salinosporamide A	1.2 ± 0.1	36.8 ± 2.4
Salinosporamide B	19.2 ± 3.5	138.7 ± 27.3
Bortezomib	3.3 ± 0.2	42.7 ± 3.4
Antiprotealide	103.6 ± 7.2	>250
Salinosporamide X3	>250	>250
Salinosporamide X5	>250	>250
Salinosporamide X7	3.6 ± 0.2	>250

[a] All assays were performed using the Z-VKM-amc substrate. Inhibitor insolubility prevented accurate IC_{50} determination at concentrations exceeding 250 μM. Data shown is the mean ± standard deviation, N = 3.

Table 4

Sequence comparison of secondary β-subunits in Actinomycetes[a]

Organism	β-subunit[b]	accession	motif 45–49	% identity[c]	E-value[d]
Salinispora tropica CNB- 440	1°, β 1	YP_001159072	MAGAA	58	NA
	2°, SalI	YP_001157868	FAGTV	100	6.0E-68
Streptomyces sp. JS360	1°	JF970179	IAGTA	52	5.0E-75
	2°, CinJ	JF970180	FAGSV	46	3.0E-71
Streptomyces avermitilis MA-4680	1°	NP_827857	IAGTA	53	7.0E-77
	2°	NP_823988	FAGTV	51	6.0E-66
Thermomonospora curvata DSM 43183	1°	YP_003299915	IAGTA	56	2.0E-76
	2°	YP_003300043	MAGTV	50	3.0E-61
Streptomyces bingchenggensis BCW-1	1°	ADI11600	IAGTL	52	9.0E-75
	2°	ADI05332	IAGTA	52	9.0E-65

[a]The two previously characterized β-subunits of *R. erythropolis* were omitted as both associate with α-subunits (25). The full sequence alignment is provided in the SI (Supplementary Figure 2).

[b]The designation of 1º is based on β-subunit association with a proteasomal gene cluster containing an α-subunit and accessory proteins, whereas 2º β-subunits are found without other proteasomal encoding genes and often cluster with natural product biosynthesis genes.

[c]Relative to SalI without prosequence.

[d]Relative to *S. tropica* β 1 without prosequence.